Asian Journal of Green Chemistry 10 (2026) 756-778

Asian Journal of Green Chemistry

Original Research Article View Article Online | View Journal

Antibacterial Activity of *Distichochlamys Orlowii* K. Larsen and M. F. Newman Essential Oil against *Streptococcus pyogenes* and *Streptococcus pneumoniae*: *In Vitro* Evidence and *In Silico* Prediction

Phan Tu Quy[1], Thanh Q. Bui[2], Nguyen Thi Thanh Hai[2], Tran Thi Ai My[2], Nguyen Duc Vu Quyen[2], Nguyen Vinh Phu[3], Nguyen Thanh Triet[4], Duong Phan Nguyen Duc[4], Ho Viet Duc[5], Nguyen Chi Bao[6], Ton That Huu Dat[7], Tran Nhat Phong Dao[8], Sunday Amos Onikanni[9,10], Nguyen Thi Ai Nhung[2*]

[1]*Department of Natural Sciences & Technology, Tay Nguyen University, Buon Ma Thuot, Dak Lak, Vietnam*
[2]*Department of Chemistry, University of Sciences, Hue University, Hue, Vietnam*
[3]*Faculty of Basic Sciences, University of Medicine and Pharmacy, Hue University, Hue, Vietnam*
[4]*Faculty of Traditional Medicine, University of Medicine and Pharmacy at Ho Chi Minh City, Ho Chi Minh City 700000, Vietnam*
[5]*Falcuty of Pharmacy, Hue University of Medicine and Pharmacy, Hue University, Hue, Vietnam*
[6]*Hue University, Hue, Vietnam*
[7]*Mientrung Institute for Scientific Research, Vietnam National Museum of Nature, Vietnam Academy of Science and Technology (VAST), Hue, Vietnam*
[8]*Faculty of Traditional Medicine, Can Tho University of Medicine and Pharmacy, Can Tho, Vietnam*
[9]*Laboratory of Experimental Endocrinology – LEEx, Institute of Biomedical Sciences, Federal University of Rio de Janeiro, Rio de Janeiro, Brazil*
[10]*Department of Chemical Sciences, Biochemistry Unit, Afe-Babalola University, Ado-Ekiti, Ekiti State, Nigeria*

ARTICLE INFORMATION

Submitted: 2025-12-01
Revised: 2026-02-18
Accepted: 2026-03-12
Published: 2026-03-19
Manuscript ID: AJGC-2512-1878
DOI: 10.48309/ajgc.2026.561172.1878

KEYWORDS

Distichochlamys orlowii
Streptococcus pyogenes
Streptococcus pneumoniae

ABSTRACT

Distichochlamys orlowii is an endemic plant from Vietnam that has been used traditionally for its medicinal properties, although its therapeutic potential has not yet been scientifically validated. This study aimed to investigate the antibacterial activity of *D. orlowii* essential oil against the respiratory pathogens *Streptococcus pyogenes* and *S. pneumoniae* using a combined experimental and *in silico* approach. The antibacterial efficacy of the essential oil was determined using minimum inhibitory concentration (MIC) assays. Its chemical profile was analyzed, and the major constituents were subsequently evaluated using computational methods, including molecular docking against the luxS protein, quantum chemical calculations, and ADMET (Absorption, Distribution, Metabolism, Excretion, Toxicity) prediction. The oil exhibited potent antibacterial activity (MICs: 64 and 128 $\mu g.mL^{-1}$). Eucalyptol, α-citral, and β-citral were identified as the primary components. Molecular docking predicted strong inhibitory potential for these compounds (binding energies ≈ -10 $kcal.mol^{-1}$). Further computational analysis highlighted the superior therapeutic properties and favorable ADMET profiles of α- and β-citral, suggesting high efficacy and low toxicity. Overall, *D. orlowii* essential oil presents a promising source for developing agents aimed at supporting respiratory health. Its major components, particularly α-citral and β-citral, are strong candidates for further research and development into novel therapeutic products.

Corresponding author, E-mail: ntanhung@hueuni.edu.vn (N.T.A. Nhung)
Tel.: +84986980263

Graphical Abstract

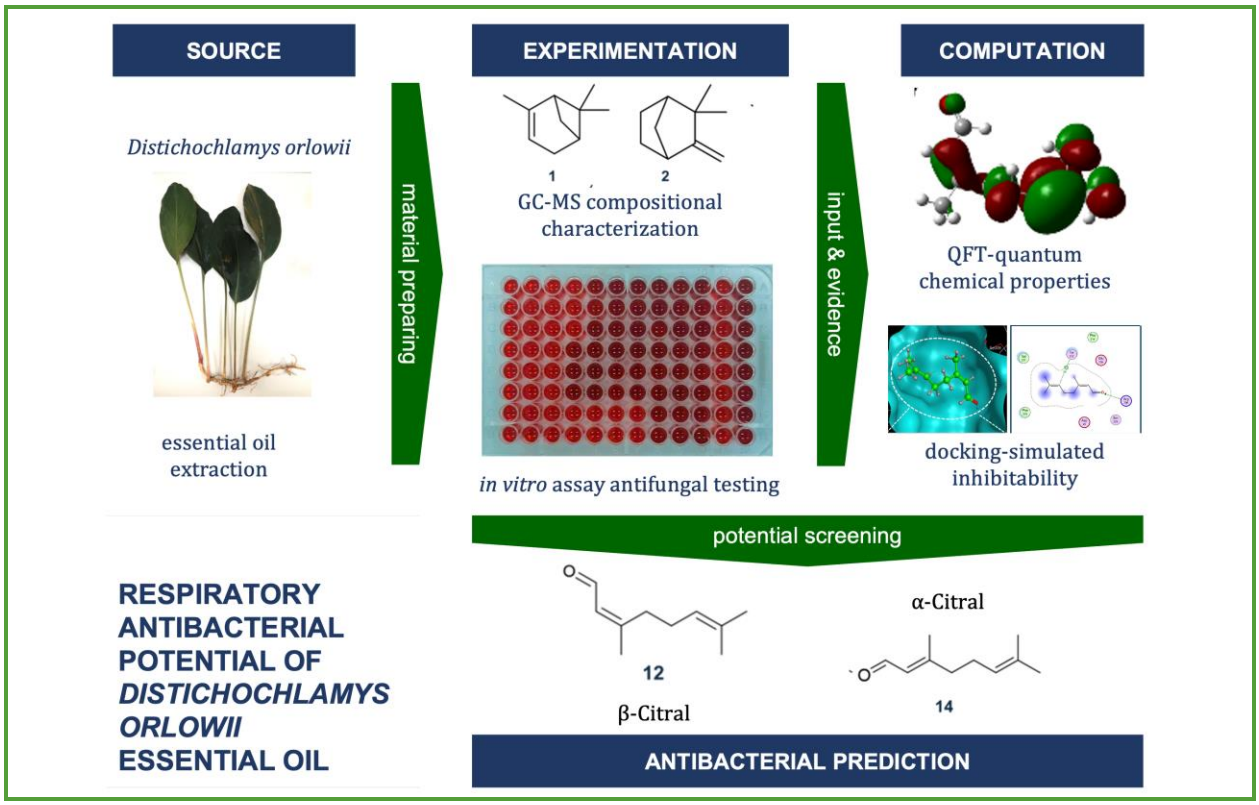

Introduction

Distichochlamys is a genus in the ginger family (Zingiberaceae), first described by M. F. Newman in 1995. To date, it comprises four known species, all endemic to Vietnam, including *D. citrea* M.F. Newman [1], *D. orlowii* K. Larsen & M.F. Newman [2], *D. rubrostriata* W. J. [3], and *D. benenica* Q. B. Nguyen & Škorničk [4]. From the traditional experience, the essential oils extracted from the plants are recognized for their distinctive aroma and have been long used as valuable and effective traditional medicines for a variety of treatments, *e.g.,* digestive disorders, inflammation-related diseases, pus removal, anti-coagulation, and wound healing. Nevertheless, knowledge of this genus remains largely confined within its endemic region (*i.e.* Vietnam) and limited primarily to traditional understanding. In the literature, there have been several attempts to characterize the chemical composition of the plant extracts, especially their essential oils, and profile their biological potentials [5-8]. The essential oil contents (v/w) were found to vary marginally between the species, *i.e.* 0.35% (*D. orlowii*), 0.25-0.60% (*D. citrea*), and 0.20% (*D. benenica*). The primary constituents of *Distichochlamys* rhizome essential oil extracts have been identified as monoterpene hydrocarbons, oxygenated monoterpenes, sesquiterpene hydrocarbons, and oxygenated sesquiterpenes. Particularly, *D. citrea* is characterized by oxygenated monoterpenes (79.4-90.7%) [1,3]; *D. benenica* is dominated by oxygenated monoterpene derivatives (ca. 75%) [6], while *D. orlowii* is known for its balanced proportions between the major components, including sesquiterpene hydrocarbons (33.7%), oxygenated monoterpenes (29.4%), monoterpene

hydrocarbons (23.9%), and oxygenated sesquiterpenes (11.2%) [8]. These phytochemical groups are widely recognized for their diverse biological and pharmacological activities. However, the therapeutic potential of *Distichochlamys* essential oil is still poorly evidenced and underreported to the literature.

Various pharmacological effects of *Distichochlamys* essential oils have been investigated and observed; yet, are still largely unexplored. For example, essential oil from *D. benenica* exhibited pronounced anti-acetylcholinesterase activity (IC_{50} 136.63 ± 2.70 µg. mL^{-1}) [6]. Furthermore, *trans-O*-coumaric acid, one of the components, has been proven to possess anti-inflammatory properties and inhibitory effects on the proliferation of several Gram-positive bacteria [5]. Considering *D. orlowii*, its therapeutic potential has attracted scientific attention only recently. Its essential oil extracts demonstrated promising hypoglycemic activity, with strong inhibition against *α*-amylase (IC_{50} 81.86 ± 0.95 µg.ml^{-1}), negligible effect on *α*-glucosidase, and no significant activity against tyrosinase [9]. Other work revealed the significant antioxidant activities of the ethanol, methanol, ethyl acetate, and dichloromethane extracts, given by scavenging free radicals DPPH (IC_{50} = 243.89 ± 5.9 to 661.42 ± 44.86 µg. mL^{-1}) and ABTS (IC_{50} = 33.58 ± 3.14 to 309.58 ± 30.46 µg. mL^{-1}) [10]. Otherwise, despite their highly promising documentation, the biological and pharmacological potential of *D. orlowii* essential oil, especially its antibacterial profiles, remains largely unexplored.

The upper respiratory tract is especially vulnerable to bacterial and viral infections due to its direct exposure to external aerosols and weak defense systems. This is more evident by the outbreak of SARS-CoV-2. In fact, a survey revealed that 94.2% of SARS-CoV-2-infected cases were also diagnosed in coinfection with other respiratory pathogens, e.g. *Streptococcus pneumoniae*, *Klebsiella pneumoniae*, *Haemophilus influenzae*, and *Streptococcus pyogenes* [5]. Especially regarding the first one, almost all patients were in severe respiratory failure and needed intensive oxygen supplementation [8]. Thus, it is essential to expand the current understanding on *Streptococcus* bacteria, particularly for the purpose of developing household supplemental natural products; this might help strengthen the respiratory resilience, ready for future harmful contagious diseases.

Streptococcus pyogenes and *Streptococcus pneumoniae* are Gram-positive bacteria in the genus *Streptococcus*. They are two of the most commonly reported with respiratory bacterial infections, more generally known as strep throat [11]. The former relates to approximately 1 million new transmitted cases annually (ca. 30% children and 10% adults), making the condition one of the most expensive healthcare burdens [12]. The latter is associated with community-acquired pneumonia and meningitis [13]. Regarding the bacterial family in general, *lux*S is considered one of the most essential proteins as it is responsible for various virulence features; this includes biofilm formation, serving imperative roles in the pathogenesis and the persistence of infections [14]. The mutation of the *lux*S gene was proven to alter significantly the virulent activity [15] and pathogenicity [16]. The well-established understanding on *lux*S suggests that the protein family can be considered as a promising target for the inhibition of *Streptococcus* contagion and colonization. The *lux*S structures of *S. pyogenes* and *S. pneumoniae* were already determined experimentally, whose corresponding crystalline assemblies are available for public referencing on the UniProtKB database under the respective entry IDs: P0C0C7 (LUXS_STRPY) and Q8DQF8 (Q8DQF8_STRR6); their structural

data provide valuable input for computational chemistry and theoretical argumentation.

By utilizing computational techniques, *in silico* research can be substantially beneficial compared to conventional lab-based (blind) screening. The advantages include reducing setting cost and increasing time productivity. Computer-aided drug design (CADD) has become more reliable over the last decades given by the enhanced algorithm sophistication; yet, at the expense of increased hardware power and software price. Fortunately, the integration of various simpler and specified platforms can provide a well-rounded view on the overall biochemopharmacological properties with equivalent to advanced reliability; the downsides should be the quality of human-based argumentation. A typical instance is molecular docking simulation for the ligand-protein complexing prediction with cost-effective advantages; yet, algorithm-simplified disadvantages; complementarily, the physicochemical properties of the potential inhibitors can solve reconcile the missing factors regarding the dynamical nature of bio-media [17,18]. Besides, quantum-calculated retrievals can provide additional views on chemophysical compatibility and electrical binding. Finally, the most promising candidates can be theoretically evaluated for their pharmacokinetic and pharmacological suitability in drug developing applications. Coupled with theoretical argument, the conclusive perspectives are of high reliability to certain further specified attempts.

In this work, *D. orlowii* essential oil was subjected to a theory-experiment combinatory study for their biopharmacological potentiality, especially against common respiratory bacteria. First, lab-based experiments were carried out for compositional profiling and antibacterial evidencing; the phytochemical characteristics were used as the input for computational iterations and theoretical arguments. Afterwards, the biochemopharmacological predictions were derived from various computer-based platforms and theory-based criteria. Finally, the most promising candidates were suggested for further testing, marking the first effort to examine *D. orlowii* antibacterial potentiality against *S. pyogenes* and *S. pneumoniae*.

Methodology

Experimental

Plant materials

D. orlowii was collected from Bach Ma National Park, Thua Thien Hue Province, Vietnam (March 2024). The species was taxonomically identified by Dr. Hoang Tan Quang (Institute of Biotechnology, Hue University). DNA-based identification was characterized using gene sequence analysis, whose results were deposited to GenBank; ID: PP538012.1. A voucher specimen (sample code: DC-10.19) was stored at Department of Chemistry, University of Sciences, Hue University. Figure 1 displays the images of *D. orlowii* plant phytomorphology (captured by the authors for this report).

Essential oil extraction

The fresh rhizomes of *D. orlowii* were cleaned (distilled water), dried (45 ± 2 °C), cut (1-2 mm), and ground into powders. The obtained powders were subjected to a steam distillation (Clevenger-type apparatus; 4 h). The extracted essential oil was dehydrated (using sodium sulfate) to the form of strong-smelling yellow liquid (0.54% w/w - essential oil to raw material). The end product was preserved in a sealed vial (10 ° C; dark space) until further analysis.

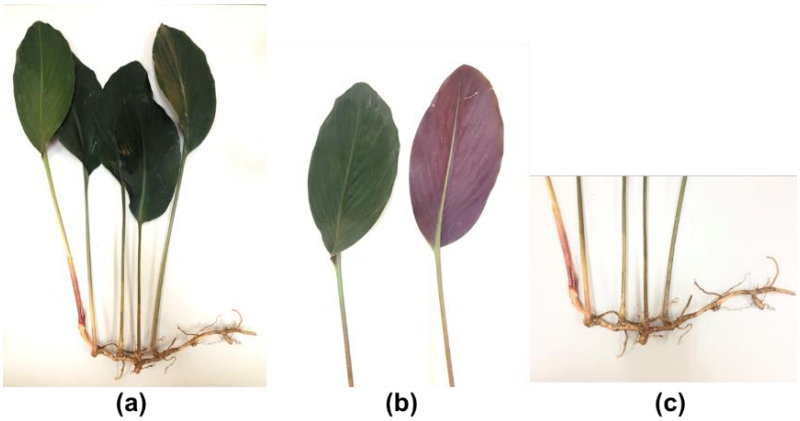

Figure 1. *D. orlowii* morphology: (a) Full body, (b) Leaves, and (c) Rhizomes (colour-printed)

Antibacterial assay

D. orlowii essential oil was tested for its antibacterial potential against *Streptococcus pyogenes* (ATCC 19615) and *Streptococcus pneumoniae* (ATCC 49619) using the broth microdilution method in 96-well microplates. The general procedure followed the instructions described by Clinical and Laboratory Standards Institute [19]. In each well, the bacterial inoculum (100 µL; 1 × 10^5 CFU/mL) and the essential oil (100 µL; a range of different concentrations) were added to each well and incubated (35 °C; 24 h). The bacterial growth was recorded 630 nm using ELx800 microplate reader (BioTek Instruments, Winooski, VT, the USA). As the references, the wells with only bacterial suspension were used as the viability control, while the wells with essential oil were used as the sterility control; the wells with bacterial suspension and Penicillin G (Sigma-Aldrich, the USA) were used as positive control. The minimum inhibitory concentrations (MICs) were determined by the lowest concentration with no bacterial growth.

Gas chromatography-mass spectrometry

D. orlowii essential oil was subjected to gas chromatography-mass spectrometry (GC-MS) using an Agilent 7890B GC system coupled with a 5975C MS detector (Agilent Technologies, USA). Separation was performed on an HP-5MS capillary column (30 m × 0.25 mm × 0.25 µm). Helium was used as the carrier gas at a constant flow rate of 1.5 $mL.min^{-1}$ (13 psi). The GC oven temperature program was as follows: initial temperature at 70 °C, followed by a linear increase to 280 °C at a rate of 10 °C. min^{-1}. The MS scanning configuration was carried out in electron ionization (EI) mode at 70 eV, with a scan range of 40-400 amu. A 1 µL sample was injected in split mode with a split ratio of 20:1. The major constituents were identified by comparison with spectra from the NIST-02 mass spectral library. All reagents, solvents, and chemicals used were of analytical grade (Sigma-Aldrich, the USA).

Computation

Input preparation

The experimental characterization in this study and the known literature provided the input for the computational implementation. Particularly, Figure 2 depicts the GC-MS-identified phytochemical formulae (compounds **1**-**19**) serving as the candidate structures for theoretical physicochemical compatibility and

bio-pharmacological suitability, while Figure 3 recites the *lux*S assemblies of *S. pyogenes* (UniProtKB: P0C0C7) and *S. pneumoniae* (UniProtKB: Q8DQF8), which were served as the representative structures for docking simulation conducted in this study. The reference compound used in this work was Penicillin G (**D**; PubChem CID 5904).

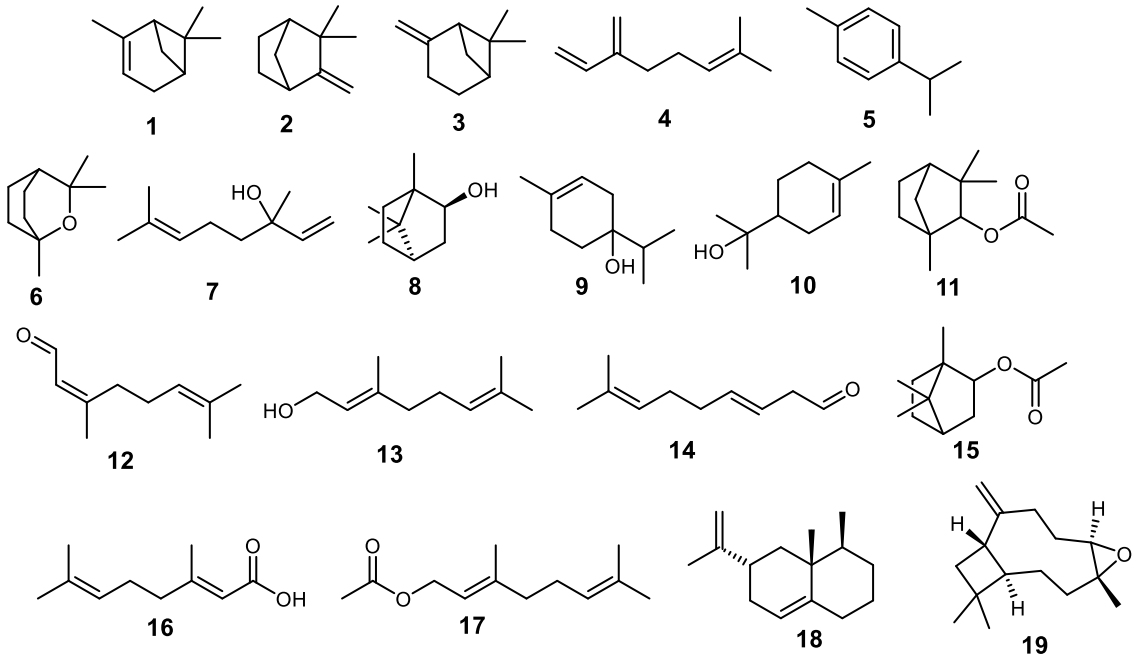

Figure 2. Structural formula of chemical components **1-19** in *D. orlowii* essential oil

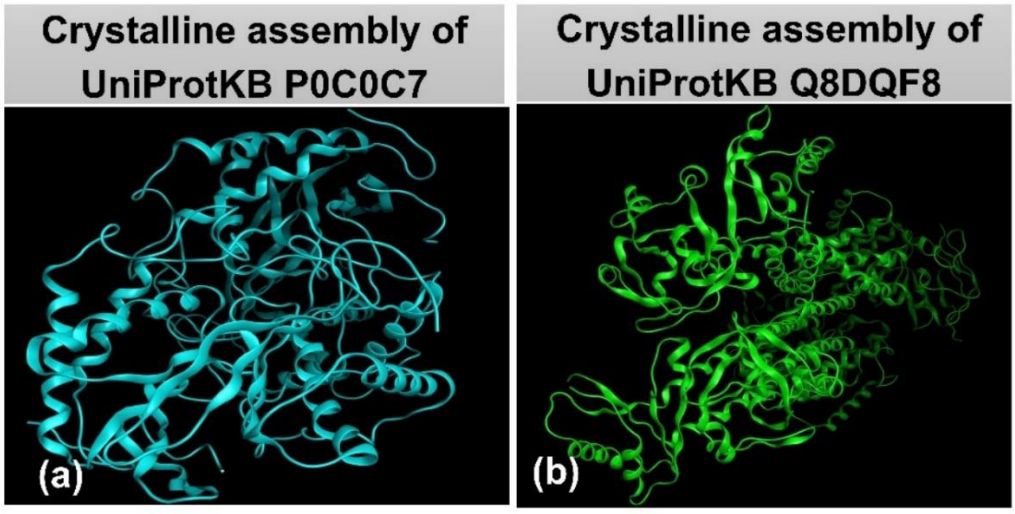

Figure 3. UniProtKB crystalline assemblies of (a) P0C0C7 (LUXS_STRPY) and (b) Q8DQF8 (Q8DQF8_STRR6)

Docking simulation

A typical procedure of molecular docking simulation (by MOE 2022.10 [20]) follows three steps, such as: (i) input preparation (configuration: protein active range 4.5 Å, ligand charge-assigning using Gasteiger-Huckel method); (ii) docking simulation (configuration: retaining poses 10; solutions per iteration 1,000; solutions per fragmentation 200); and (iii) re-docking iteration (threshold: root-mean-square deviation (RMSD) values < 2 Å; recommended by MOE). In theory, the docking score (DS) energy of the associated inhibitory system represents a pseudo-Gibbs free energy, RMSD values and number of hydrogen-like interactions are referred to bio-conformational rigidity and binding strength, respectively; thereby, they are considered as the primary parameters for inhibitory effectiveness. In technique, MOE can render ligand-protein interaction maps (2D) and in-pose arrangements (3D) for further evaluation on the spatial complementarity.

Quantum calculation

Molecular quantum calculation (by Gaussian 09 [21]) using density functional theory (DFT) can efficiently provide chemical properties of the investigated structures. In particular, level of theory M052X/6–311++G(d,p) and basis set def2-TZVPP [22] were selected. The converged geometries were examined for the structural global minimum on the potential energy surface (PES) by vibrational frequencies. The frozen-core approximation for non-valence-shell electrons was applied. The resolution-of-identity (RI) approximation was set. The frontier orbital analysis was carried out by NBO 5.1 at the level of theory M052X/def2-TZVPP [23].

Physicochemical analysis

The drug likeness of the phytochemicals was predicted by a combinational model. The parameters were the physical properties retrieved from MOE 2022.10 database [20,24]; the model was based on Gasteiger–Marsili method [25] and now integrated as a sub-function in MOE 2022.10. The theoretical criteria were from Lipinski's rule of five [26], which provides the theoretical criteria for a well membrane-permeable candidate, *i.e.* molecular mass < 500 amu; hydrogen bond donors ≤ 5; and hydrogen bond acceptors ≤ 10; logP < +5 [27,28].

ADMET analysis

The pharmacological potentiality of the candidates was assessed by a combinational model. The parameters were ADMET (absorption, distribution, metabolism, excretion, and toxicity) properties retrieved from SwissADME (Swiss Institute of Bioinformatics; http://www.swissadme.ch/; 30th August 2024). The theoretical standards were from Pires' interpretations [29].

Results and Discussion

Experimental findings

Antibacterial evidence

The assay setting was captured to Figure 4, whose results are recorded and summarized into Table 1. In overall, *D. orlowii* essential oil exhibited noticeably significant antibacterial activity against the two tested microorganism pathogens *S. pyogenes* and *S. pneumoniae* by the respective concentrations 64 and 128 μg. mL^{-1}.

The commercial antibiotic, *i.e.* Penicillin G, was recorded for MICs value at 0.5 µg. mL^{-1}. Notably, this is the first time the antibacterial activity of this plant has been reported, especially regarding these two respiratory bacteria. Preliminarily, this observable is solid evidence for the biological potentials of *D. orlowii* essential oil components, thus reasoning for further attempts to determine the component-activity relationship.

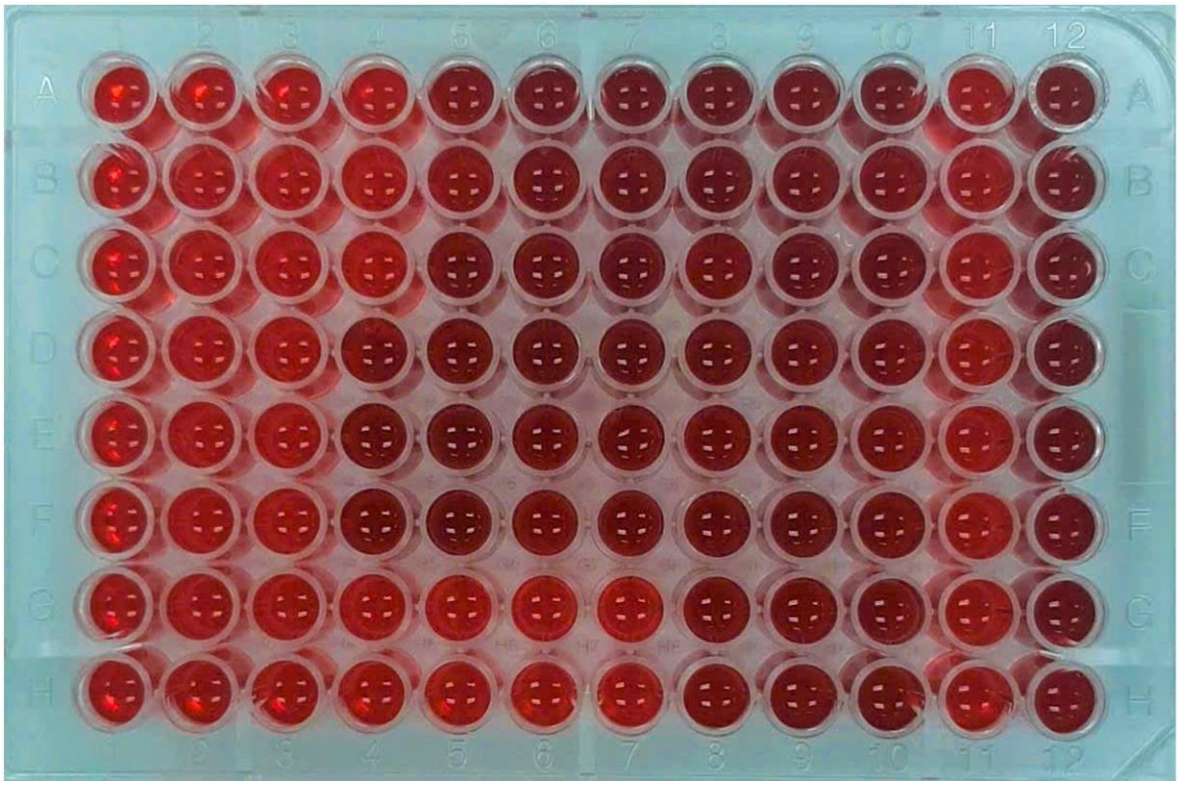

Figure 4. Bioassay settings for *D. orlowii* essential oil antibacterial testing (colour-printed)

Table 1. *In vitro* results for the antibacterial activities of *D. orlowii* essential oil against *S. pyogenes* and *S. pneumoniae*

Essential oil concentration (µg. mL^{-1})		**512**	**256**	**128**	**64**	**32**	**16**	**8**	**4**	**2**	**1**	**(-)**	**(+)**
D. orlowii sample		1	2	3	4	5	6	7	8	9	10	11	12
S. pyogenes	A	-	-	-	-	+	+	+	+	+	+	-	+
S. pyogenes	B	-	-	-	-	+	+	+	+	+	+	-	+
S. pyogenes	C	-	-	-	-	+	+	+	+	+	+	-	+
S. pneumoniae	D	-	-	-	+	+	+	+	+	+	+	-	+
S. pneumoniae	E	-	-	-	+	+	+	+	+	+	+	-	+
S. pneumoniae	F	-	-	-	+	+	+	+	+	+	+	-	+
Penicillin G	G	-	-	-	-	-	-	-	+	+	+	-	+
Penicillin G	H	-	-	-	-	-	-	-	+	+	+	-	+
PG concentration		32	16	8	4	2	1	0.5	0.25	0.125	0.0625	(-)	(+)

Chemical composition

The total ion chromatogram obtained from GC-MS analysis is demonstrated in Figure 5, whose data are extracted and summarized into Table 2. In general, the results revealed a diverse composition with 19 compounds detected (denoted as **1**-**19**), accounting for ca. 95% of the total *D. orlowii* essential oil. The predominant component is eucalyptol (**6**; 27.81%), which has been consistently reported for a diversity of biological potentials such as antibacterial, anti-inflammatory, anticancer, and antitumor activities [30-32]; it is followed by *α*-citral (**14**; 17.13%) and *β*-citral (**12**; 13.91%). This compositional pattern is also consistent with the previous findings in the literature on other *Distichochlamys* species; for a typical example regarding eucalyptol: *D. citrea* (23.00% to 43.67%), *D. rubrostriata* (13.20% to 22.00%), and *D. benenica* (54.39%) [6,7,33,34]. Besides, the other considerable constituents include geranyl acetate (**17**; 6.98%), *β*-pinene (**3**; 4.89%), geraniol (**13**; 4.79%), and aristolochene (**18**; 4.36%), whose proportions are ca. 5%. Interestingly, aristolochene was also found in *D. orlowii* essential oil. This bicyclic sesquiterpene was especially characterized to the essential oil extracted from *Aristolochia indica* Linn. aerial components (Aristolochiaceae family) [35,36]. Furthermore, *p*-cymene, endo-borneol, borneol acetate, and geranic acid were initially reported for their existence in *D. orlowii* essential oil; the

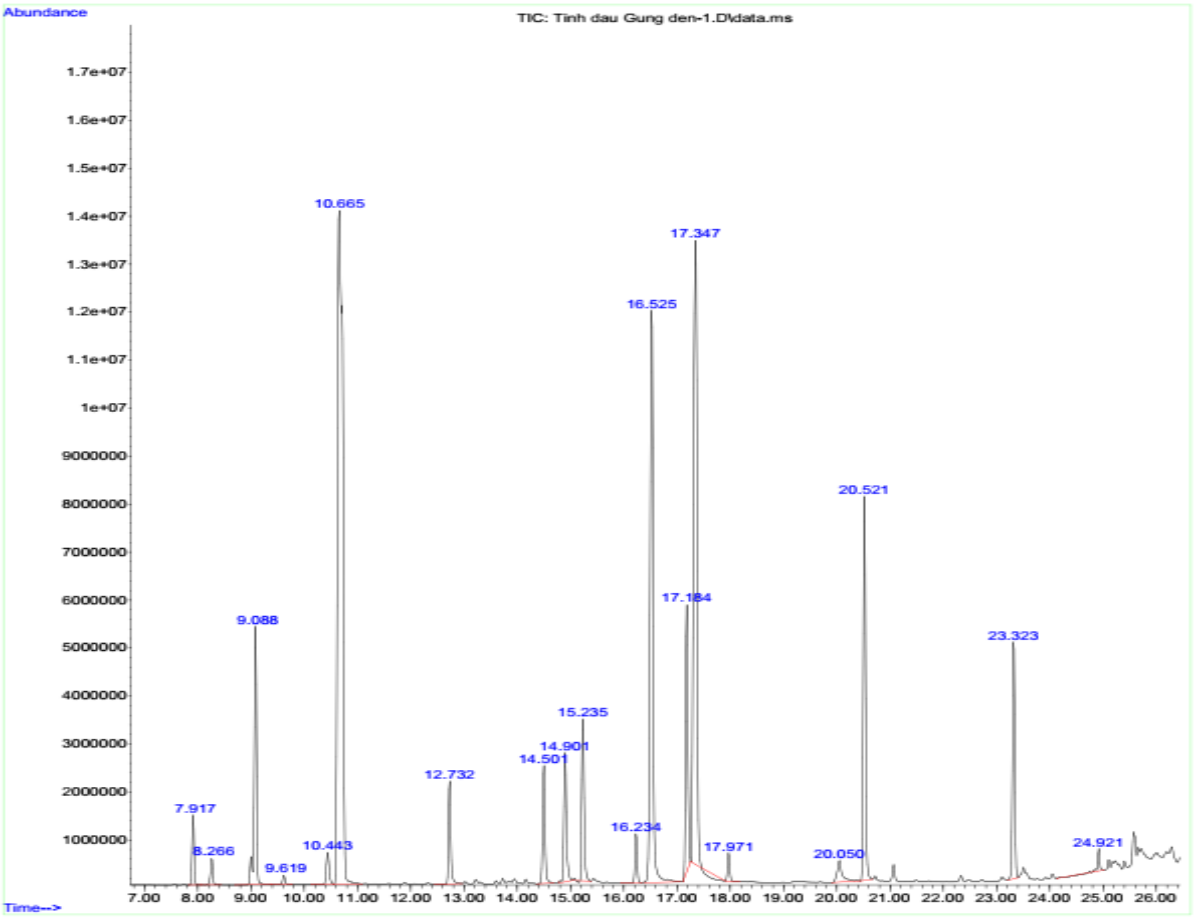

Figure 5. Total gas-chromatography spectrum of *D. orlowii* essential oil

Table 2. Identification of bioactive compounds in *D. orlowii* essential oil

Notation	Retention time (min)	Compound	Formula	Class	Percentage (%)	
					This work	Literature
1	7.917	α-Pinene	$C_{10}H_{16}$	Mh	1.12	0.9-2.2
2	8.266	Camphene	$C_{10}H_{16}$	Mh	0.49	2.8
3	9.088	β-Pinene	$C_{10}H_{16}$	Mh	4.89	9.0
4	9.619	β-Myrcene	$C_{10}H_{16}$	Mh	0.16	0.8
5	10.443	p-Cymene	$C_{10}H_{14}$	Mh	0.68	-
6	10.665	Eucalyptol	$C_{10}H_{18}O$	Om	27.81	7.6
7	12.732	Linalool	$C_{10}H_{18}O$	Om	1.84	0.6-3.1
8	14.501	endo-Borneol	$C_{10}H_{18}O$	Om	2.25	-
9	14.901	Terpinen-4-ol	$C_{10}H_{18}O$	Om	2.54	2.9
10	15.235	α-Terpineol	$C_{10}H_{18}O$	Om	3.04	0.1
11	16.234	Fenchyl acetate	$C_{12}H_{20}O_2$	Om	0.85	0.1-0.15
12	16.535	β-Citral	$C_{10}H_{16}O$	Om	13.91	4.6-12.6
13	17.184	Geraniol	$C_{10}H_{18}O$	Om	4.79	0.9-2.4
14	17.971	α-Citral	$C_{10}H_{16}O$	Om	17.13	11.9
15	20.050	Bornyl acetate	$C_{12}H_{20}O_2$	Om	0.50	-
16	20.521	Geranic acid	$C_{10}H_{16}O_2$	Om	0.87	-
17	23.323	Geranyl acetate	$C_{12}H_{20}O_2$	Om	6.98	1.4-16.5
18	23.323	Aristolochene	$C_{15}H_{24}$	Sh	4.36	15.2
19	24.921	Caryophyllene oxide	$C_{15}H_{24}O$	Mh	0.32	2.7
		Total			94.53	
		Monoterpene hydrocarbons (Mh)			7.66	
		Oxygenated monoterpenes (Om)			82.51	
		Sesquiterpene hydrocarbons (Sh)			4.36	

contents of camphene, β-pinene, β-myrcene, aristolochene, and caryophyllene oxide were found to be lower than those reported in the previous studies, while the corresponding values for eucalyptol, α-citral, and geraniol are noticeably higher. This can be explained by the differences in harvesting area, material age, or extraction process, which are commonly seen in natural product research. From the logical argument, the major compounds (considerably over 5%) are likely to be responsible for the observable total antifungal properties evidenced by the *in vitro* assays. Thus, their contributive footages on the biological activities are of necessity for further research. Reasonably, they are to be in special consideration by *in silico* prediction. Otherwise, the minor parts (speculatively under 5%) are low-likely to have a significant contribution, thus to receive less attention.

Computational retrievals

Protein-structure inhibitability

Generally, the phytochemicals (compounds **1**-**19**) can be evaluated for their intermolecular affinity towards protein structures using molecular docking technique. In this work, the assemblies for *lux*S proteins of *S. pyogenes* (P0C0C7) and *S. pneumoniae* (Q8DQF8) were selected as the representatives for the attempt to reach the preliminary insight into the ligand-

protein inhibitability, rather than the conclusion on the antibacterial inhibition. Typically, the most effective ligand-binding site was identified and selected by MOE default algorithm; the primary parameters are the total docking score (*i.e.* a pseudo-Gibbs free energy) and the number of hydrogen-like bonds (aka. strong hydrophilic interactions).

The results for each ligand-protein duo are extracted from the docking-based simulations and summarized in Table 3. Overall, the candidates perform upper-moderate inhibitory potentials toward the selected structures with no pronounced differences given their corresponding docking-score values.

Table 3. Screening results on inhibitability of compounds **1-19** and **D** toward the sites of P0C0C7 and Q8DQF

Complex		Site 1		Site 2		Site 3		Site 4		Site 5		Average
P	**L**	**E**	**N**	**E**	**N**	**E**	**N**	**E**	**N**	**E**	**N**	**E**
P0C0C7	1	-7.2	0	-7.0	0	-8.7*	1*	-6.8	0	-6.0	0	-7.1
	2	-8.0	0	-9.0*	1*	-7.7	0	-7.0	0	-6.5	0	-7.6
	3	-7.1	0	-6.8	0	-8.3*	1*	-6.3	0	-6.0	0	-6.9
	4	-7.4	0	-7.0	0	-6.7	0	-6.3	0	-8.8*	1*	-7.2
	5	-7.0	0	-7.3	0	-8.6*	1*	-7.8	1	-6.9	0	-7.5
	6	-10.3*	2*	-8.7	1	-8.0	0	-7.6	0	-7.9	0	-8.5
	7	-9.0	1	-10.9*	2*	-8.9	1	-7.5	0	-7.0	0	-8.7
	8	-8.7	1	-11.7*	3*	-8.0	1	-7.6	0	-7.4	0	-8.7
	9	-8.6	0	-10.7*	2*	-7.4	0	-9.0	1	-7.1	0	-8.6
	10	-7.7	1	-6.9	0	-7.0	0	-10.4*	2*	-8.8	1	-8.2
	11	-10.8	2	-12.3*	4*	-9.2	1	-8.8	1	-9.0	1	-10.0
	12	-10.6*	2*	-9.5	1	-8.0	0	-7.4	0	-7.0	0	-8.5
	13	-10.8*	2*	-9.3	1	-9.0	1	-8.0	0	-7.6	0	-8.9
	14	-10.3*	2*	-8.7	1	-7.3	0	-6.8	0	-6.5	0	-7.9
	15	-12.6*	4*	-10.8	2	-9.4	1	-8.9	1	-8.5	1	-10.0
	16	-9.0	1	-8.9	1	-11.3*	3*	-8.6	1	-7.3	0	-9.0
	17	-8.9	1	-11.4*	3*	-9.6	1	-8.0	0	-7.5	0	-9.1
	18	-10.5*	2*	-9.0	1	-8.7	1	-8.5	1	-7.0	0	-8.7
	19	-7.3	0	-8.0*	1*	-7.0	0	-6.7	0	-6.9	0	-7.2
	D	-10.9	2	-12.8*	4*	-9.0	1	-8.6	1	-8.9	1	-10.0
Q8DQF8	1	-7.5	0	-8.2*	1*	-7.0	0	-6.8	0	-6.5	0	-7.2
	2	-7.1	0	-8.0*	1*	-6.7	0	-6.5	0	-6.8	0	-7.0
	3	-6.7	0	-8.4*	1*	-7.0	0	-7.3	0	-6.8	0	-7.2
	4	-7.7	0	-8.7*	1*	-7.1	0	-6.9	0	-6.3	0	-7.3
	5	-9.2*	1*	-8.2	0	-7.4	0	-7.2	0	-6.7	0	-7.7
	6	-9.4*	1*	-7.2	0	-7.0	0	-6.9	0	-6.2	0	-7.3
	7	-10.8*	2*	-8.1	1	-7.1	0	-6.3	0	-6.5	0	-7.8
	8	-8.8*	1*	-6.9	0	-7.2	0	-7.7	0	-7.0	0	-7.5
	9	-8.5*	1*	-7.6	0	-7.1	0	-6.4	0	-6.8	0	-7.3
	10	-8.2	0	-9.3*	1*	-7.8	0	-7.4	0	-7.0	0	-7.9
	11	-9.1*	1*	-8.0	0	-8.3	0	-7.5	0	-7.2	0	-8.0
	12	-8.7	1	-11.8*	3*	-8.3	1	-7.2	0	-7.4	0	-8.7
	13	-10.5*	2*	-9.0	1	-8.1	0	-7.3	0	-7.1	0	-8.4
	14	-8.7*	1*	-6.9	0	-6.5	0	-6.0	0	-6.2	0	-6.9
	15	-8.9*	1*	-7.0	0	-6.7	0	-6.3	0	-6.5	0	-7.1
	16	-10.7*	2*	-9.0	1	-8.7	1	-7.2	0	-6.3	0	-8.4
	17	-8.8	1	-10.9*	2*	-7.5	0	-9.0	1	-7.3	0	-8.7
	18	-7.2	0	-9.3*	1*	-7.0	0	-6.7	0	-6.4	0	-7.3
	19	-8.3	1	-9.0*	1*	-7.2	0	-6.9	0	-7.0	0	-7.7
	D	-13.0*	6*	-10.2	3	-9.8	2	-9.0	1	-8.5	1	-10.1

*P: Protein; L: Ligand; E: DS value (kcal.mol^{-1}); and N: Hydrogen bond count; *most stable inhibitory complex duo.*

If strictly following the theoretical interpretations, the most stable inhibitory structures can be: 11-P0C0C7 ($\overline{DS}$ -10.0 kcal.mol^{-1}; DS_{max} -12.3 kcal.mol^{-1}, hydrogen bond count 4) and 15-P0C0C7 ($\overline{DS}$ -10.0 kcal.mol^{-1}; DS_{max} -12.6 kcal.mol^{-1}, hydrogen bond count 4) regarding *S. pyogenes* representative; or, 12-Q8DQF8 ($\overline{DS}$ -8.7 kcal.mol^{-1}; DS_{max} -11.8 kcal.mol^{-1}, hydrogen bond count 3) and 17-Q8DQF8 ($\overline{DS}$ -8.7 kcal.mol^{-1}; DS_{max} -10.9 kcal.mol^{-1}, hydrogen bond count 2) regarding *S. pneumoniae* representative.

Most of these ligands are not either the primary components in *D. orlowii* essential oil or express a predominant figure. Regarding the respiratory subjects, these values are comparable to the findings from the previous research on *D. citrea* M.F. Newman (another *Distichochlamys* species) [37], yet significantly inferior to the organosulfur compounds extracted from garlic [38]. This is understandable as either garlic or organosulfur compounds are well-known natural sources for their antimicrobial effects by both folk experience and scientific knowledge. From the theory-to-experiment perspective, the docking-retrieved inhibitability is of high consistency with the assay-observed inhibition regarding the both moderate evaluations. Finally, no apparent differences in interacting potentiality means the candidates are likely to relate their biological activities to their physicochemical compatibility.

The descriptions for in-site configurations of the most effective inhibitory systems are illustrated into Figures 6 and 7 (ligand-P0C0C7and ligand-Q8DQF8, respectively). Except for 11-P0C0C7 and 15-P0C0C7, most ligand-protein complexes do not heavily rely on the hydrophilic interactions for their formation given by the hydrogen bond counts only 1-2. In contrast, the van der Waals contribution seems to be more apparently given the numbers of involved amino acids detected. The 3D images indicate that there seems to be no noticeable structural or spatial constraints for the ligand-protein bindings; this is expected since the compounds have small and simple chemical characteristics.

Quantum chemical property

In particular, the potential inhibitors (compounds 1-19) can be evaluated for their bio-medium compatibility and interactive tendency using the molecular quantum analysis. The calculated properties are intrinsic to the input structures and do not require an external structure for reference (such as docking simulation). The optimal geometries derived by the DFT method are demonstrated in Figure 8. In general, the input structures converge smoothly through self-consistent iterations without any noticeable bonding abnormality (such as angles and lengths). This computer-based convenience is consistent with the nature-existed stableness (of the natural products in general). In fact, theoretical compounds often undergo the self-consistent processes with geometric constraints, *e.g.,* transition-metal tetrylone complexes [39].

Table 4 summarizes the ground state energy and the dipole moment characterized for each structure, which correspond to the molecular chemical reactivity and the dipole-dipole interactability, respectively. Given bio-inhibitory applicability, lower values of the former means that the host molecules are predicted to more likely retain their chemical characteristics during the bio-medium transport before approaching their targeted biological structures, also preserving the reliability of other theoretical predictions. This perspective indicates the appropriateness of all structures as the all possess negative corresponding values; more particularly, the most favored candidates are compounds **11**, **15**, **17**, and **19** (ground-state energy < 600 a.u.).

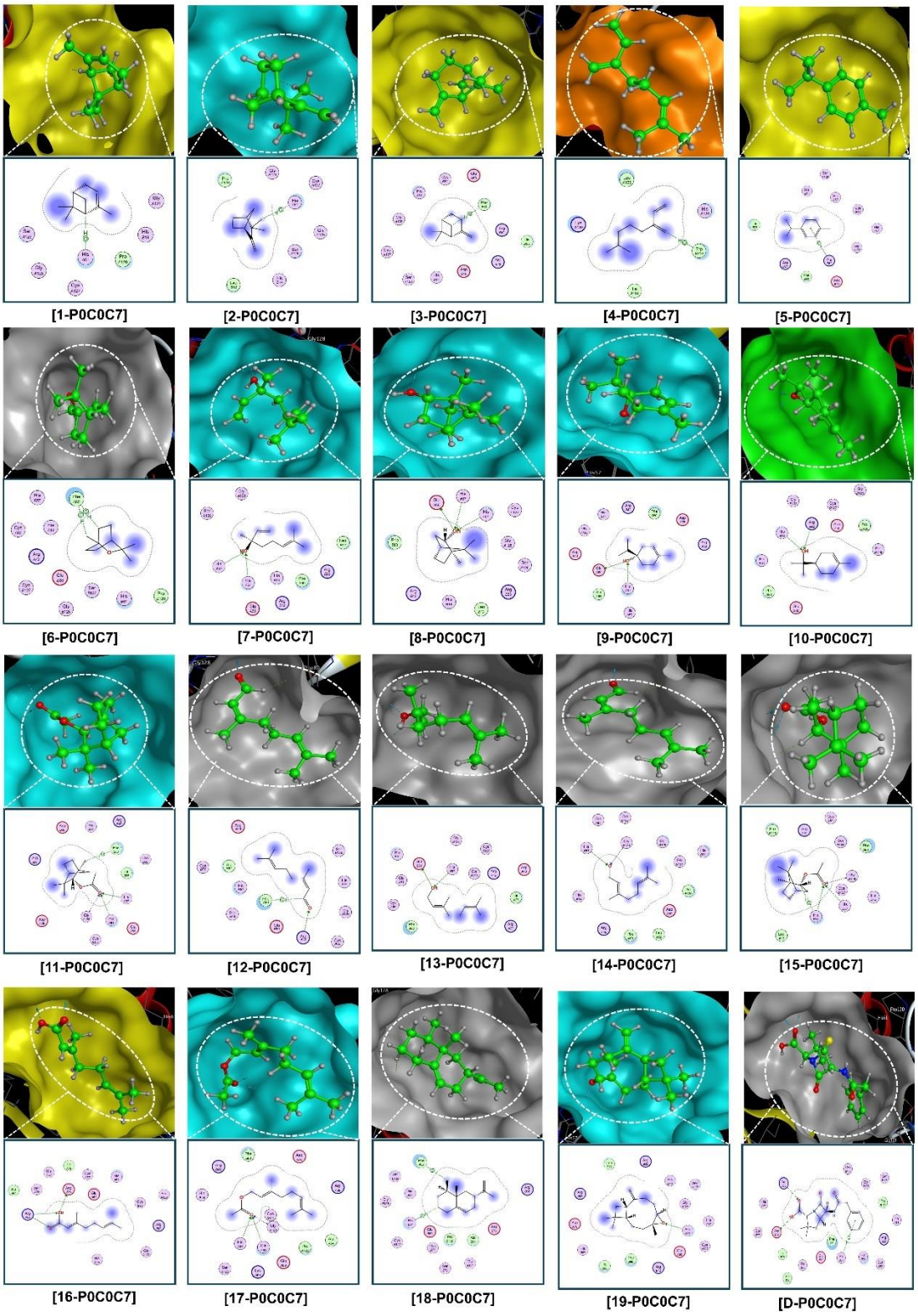

Figure 6. Visual presentation and in-pose interaction map of ligand-P0C0C7 inhibitory structures (ligand: **1-19** and controlled drug: **D**); dashed arrow: hydrogen-like bonding, blurry purple: van der Waals interaction, and dashed contour: conformational fitness (colour-printed)

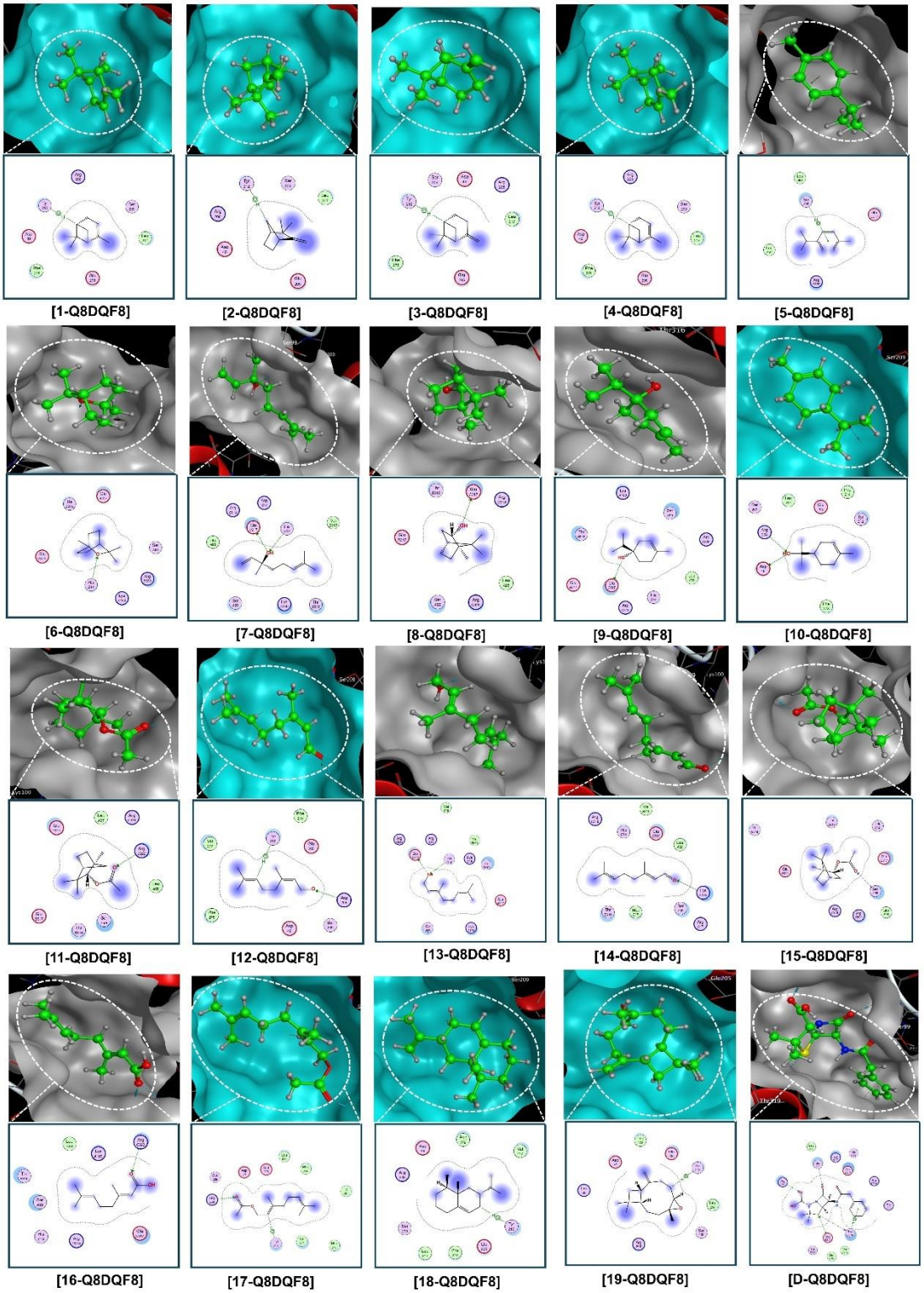

Figure 7. Visual presentation and in-pose interaction map of ligand-Q8DQF8 inhibitory structures (ligands **1-19** and controlled drug **D**); dashed arrow: hydrogen-like bonding, blurry purple: van der Waals interaction, and dashed contour: conformational fitness (colour-printed)

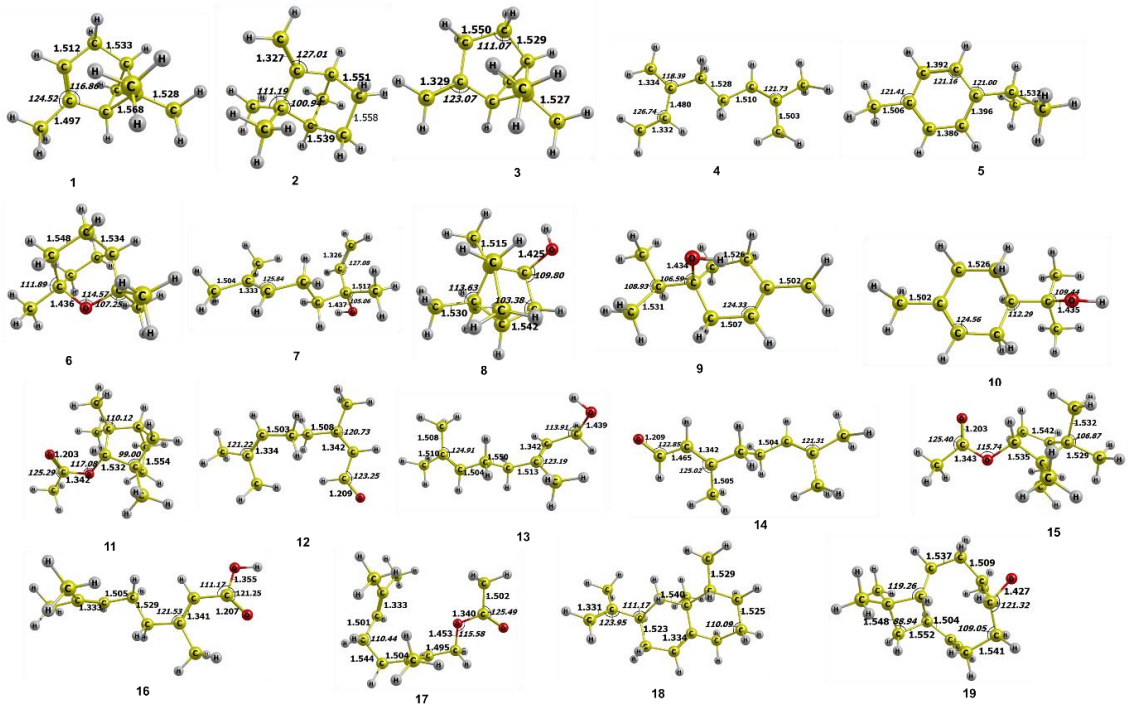

Figure 8. Geometrically optimal structures of ligands **1-19**; length (Å), angle (°) (colour-printed)

Table 4. Ground state electronic energy and dipole moment values of compounds **1-19**

Compound	Ground state electronic energy (a.u.)	Dipole moment (D)
1	-390.71	0.19
2	-390.73	0.66
3	-390.71	0.72
4	-390.67	0.75
5	-389.55	0.05
6	-467.21	1.60
7	-467.15	1.92
8	-467.20	1.61
9	-467.19	1.81
10	-467.19	1.69
11	-619.89	2.01
12	-465.94	4.56
13	-467.23	2.07
14	-465.94	5.18
15	-619.89	2.02
16	-541.22	2.39
17	-619.83	2.69
18	-586.11	0.69
19	-661.30	2.47

Given bio-medium compatibility, higher values of the latter means that the host molecules are expected less likely to be resisted by a dipole-solvent environment, such as of living organisms. This point unfavorably opts against the consideration of compounds **1**-**5** and **18** (dipole moment < 1 D), while especially opts for the selection of compound **12** (4.56 D) and compounds **14** (5.18 D), which are also the major constituents in *D. orlowii* essential oil.

Figure 9 displays the frontier molecular orbitals of the studied structures. Theoretical understanding suggests that the highest occupied molecular orbital (HOMO) represents the region of electron-donation tendencies, while the lowest unoccupied molecular orbital (LUMO) indicates the opposite counterparts [40,41]. This can be helpful in some cases when determining the dominant tendencies; for typical example, it is rather transparent that compounds **1**, **15**, or **18** should have stronger electron-donating tendencies since their lowest virtual orbitals are negligible. Regarding the gap energy, values within the range of insulation and semi-conduction (3.2 eV < ΔE_{GAP} < 9 eV [42]) are considered favorable. These structures are believed to have the potential to induce electric binding with polypeptide structures, *e.g.,* proteins, enzymes, and certain hormones, which were reported with [43] and explained for their electric conductivity [44]. Except for those with particularly over-threshold values such as compounds **11** and **15** (ΔE_{GAP} ca. 10 eV), most others are appropriate. Further, **6** (9.020 eV), **12** (7.625 eV), and **14** (7.614 eV) are considered promising from the standpoint of electrical interaction, especially the latter two.

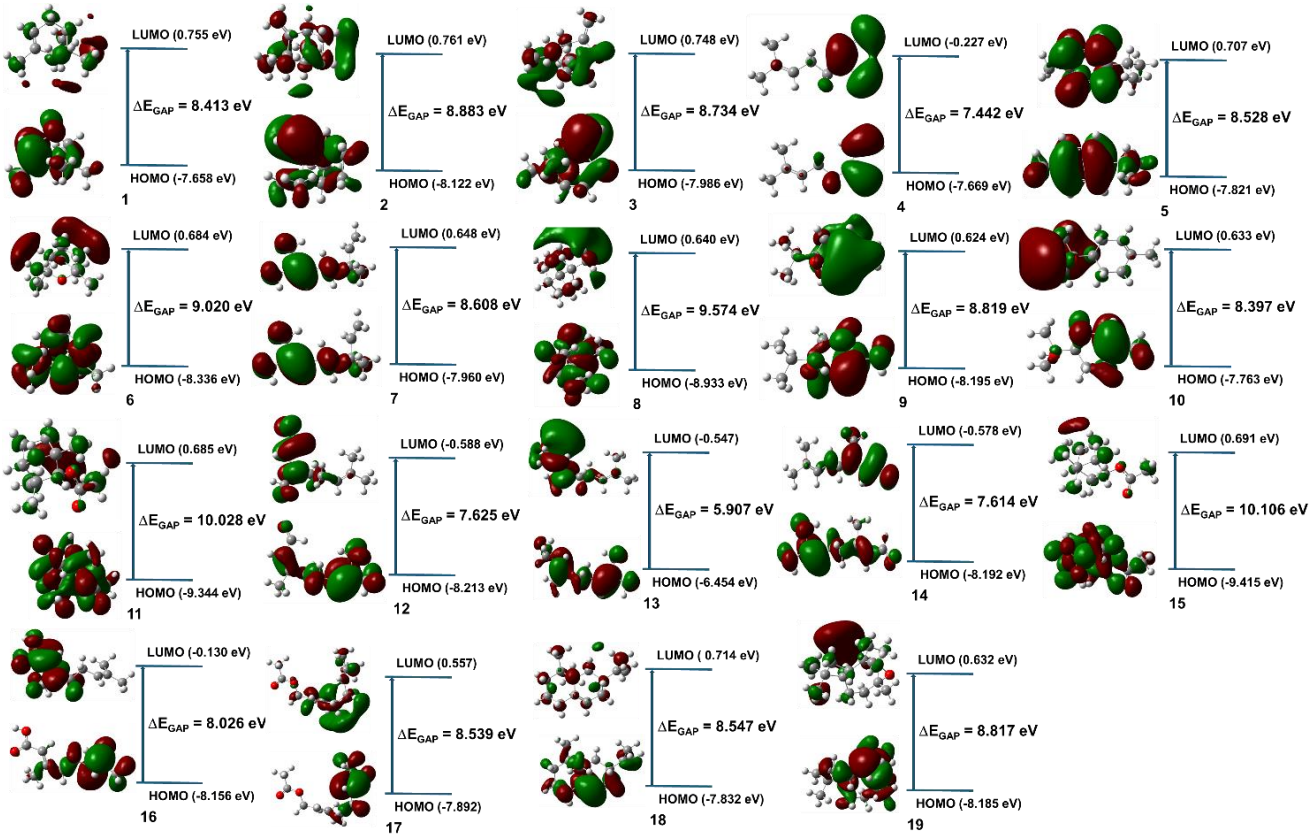

Figure 9. HOMO and LUMO of compounds **1-19**; red: positive sign of the original wavefunction and green: the negative sign of the original wavefunction (colour-printed)

Physicochemical compatibility

The physical properties of the studied compounds (**1**-**17**) were summarized in Table 5, including molecular mass (amu), polarizability (Å^3), size (Å), and dispersion coefficients (logP and logS). These parameters are evaluated for their drug likeness based on Lipinski's rule of five. The overall preview suggests that all the compounds well satisfy all the criteria; in particular, the heaviest figure is 220.4 amu (compound **19**), the largest number of hydrogen bond count is 4 (compounds **11** and **15**), and the most positive logP value is +4.25 (compound **19**).

Besides, the polarizability is considered as an important indicator as it represents the sensitivity of the host molecule to external electric fields [45], which can be in turn induced by polarized structures such as amino acid-based enzymes. This means higher polarizability might be conducive to the protein inhibiting applications. From this argument, compound **18** (25.7 Å^3) and compound **19** (26.4 Å^3) are regarded as the most promising inducers given by the highest corresponding values. Furthermore, their negative-inclined logS values implicate the limited aqueous solubility of the compounds, which are expectable as they are all *D. orlowii* oil-based constituents. Considering those with the highest percentages, compound **6** (154.3 amu; 18.9 Å^3; logP 2.81), compound **12** (152.3 amu; 18.4 Å^3; logP 2.56), and compound **14** (152.3 amu; 19.5 Å^3; logP 2.71) fall in within the range of good physicochemical compatibility.

Table 5. Physicochemical properties of compounds **1**-**19** and **D**

Compound	Mass (amu)	Size (Å)	Polarisability (Å^3)	Dispersion cefficients		Hydrogen bond* (Q8DQF8/P0C0D7)
				(logP)	(logS)	
1	136.3	257.9	16.4	2.89	-2.63	1/1
2	136.3	256.3	17.9	2.83	-2.49	1/1
3	136.2	254.8	18.3	3.01	-2.73	1/1
4	136.2	295.2	19.2	2.86	-2.58	1/1
5	134.2	257.8	18.1	3.74	-3.02	0/1
6	154.3	282.1	18.9	2.81	-2.38	2/1
7	154.3	298.8	20.2	2.39	-1.91	2/2
8	154.3	262.0	17.2	2.19	-2.57	3/1
9	154.3	283.1	16.8	2.03	-1.87	2/1
10	154.3	275.6	19.5	2.29	-2.37	2/2
11	196.3	325.2	20.8	3.08	-2.71	4/1
12	152.3	295.2	18.4	2.56	-2.29	2/3
13	152.3	295.4	19.9	2.58	-1.65	2/2
14	152.3	295.8	19.5	2.71	-2.29	2/1
15	196.3	324.2	22.1	3.35	-3.13	4/1
16	168.3	293.8	20.3	2.69	-2.78	3/2
17	196.3	360.7	22.8	3.31	-2.58	3/2
18	204.4	379.9	25.7	4.04	-3.82	2/1
19	220.4	372.1	26.4	4.25	-4.06	1/1
D	334.5	390.7	32.1	2.69	-2.19	4/6

**Counted from docking results of each most effective ligand-protein inhibitory complex*

Pharmacological suitability

The ADMET properties of the compounds are summarized in Table 6 (compounds **1**-**10**) and Table 7 (compounds **11**-**19**), categorized into absorption, distribution, metabolism, excretion, and toxicity. These parameters are evaluated for their pharmacological suitability based on Pires' interpretations. All the candidates can be effectively transported and absorbed via intestinal routine (over 90%) with considerably high $CaCo_2$ permeability (logPapp ca. 10^{-6}). Additionally, they do not have noticeable effects on the extrusive activities of the P-glycoprotein family.

Table 6. ADMET properties of the studied compounds **1-10**

Property	1	2	3	4	5	6	7	8	9	10	Unit
Absorption											
Water solubility	-3.733	-4.34	-4.191	-4.497	-4.081	-2.63	-2.612	-2.462	-2.296	-2.039	(1)
$CaCo_2$ permeability	1.38	1.387	1.385	1.4	1.527	1.485	1.493	1.484	1.502	1.489	(2)
Intestinal absorption	96.041	94.148	95.525	94.696	93.544	96.505	93.163	93.439	94.014	94.183	(3)
Skin Permeability	-1.827	-1.435	-1.653	-1.043	-1.192	-2.437	-1.737	-2.174	-2.182	-2.418	(4)
P-glycoprotein substrate	No	No	No	No	No	Yes	No	No	No	Yes	(5)
P-glycoprotein I inhibitor	No	No	No	No	No	No	No	No	No	No	(5)
P-glycoprotein II inhibitor	No	No	No	No	No	No	No	No	No	No	(5)
Distribution											
VDss	0.667	0.547	0.685	0.363	0.697	0.491	0.152	0.337	0.21	0.207	(6)
Fraction unbound	0.425	0.354	0.35	0.39	0.159	0.553	0.484	0.486	0.514	0.565	(6)
BBB permeability	0.791	0.787	0.818	0.781	0.478	0.368	0.598	0.646	0.563	0.305	(7)
CNS permeability	-2.201	-1.71	-1.857	-1.902	-1.397	-2.972	-2.339	-2.331	-2.473	-2.807	(8)
Metabolism											
CYP2D6 substrate	No	No	No	No	No	No	No	No	No	No	(5)
CYP3A4 substrate	No	No	No	No	No	No	No	No	No	No	(5)
CYP1A2 inhibitor	No	No	No	No	Yes	No	No	No	No	No	(5)
CYP2C19 inhibitor	No	No	No	No	No	No	No	No	No	No	(5)
CYP2C9 inhibitor	No	No	No	No	No	No	No	No	No	No	(5)
CYP2D6 inhibitor	No	No	No	No	No	No	No	No	No	No	(5)
CYP3A4 inhibitor	No	No	No	No	No	No	No	No	No	No	(5)
Excretion											
Total clearance	0.043	0.049	0.03	0.438	0.239	1.009	0.446	1.035	1.269	1.219	(9)
Renal OCT_2 substrate	No	No	No	No	No	No	No	No	No	No	(5)
Toxicity											
AMES toxicity	No	No	No	No	No	No	No	No	No	No	(5)
Max. tolerated dose	0.48	0.305	0.371	0.617	0.903	0.553	0.774	0.577	0.857	0.886	(10)
hERG I inhibitor	No	No	No	No	No	No	No	No	No	No	(5)
hERG II inhibitor	No	No	No	No	No	No	No	No	No	No	(5)
Oral Rate Acute Toxicity	1.77	1.554	1.673	1.643	1.827	2.01	1.704	1.707	1.811	1.923	(11)
Oral rate chronic toxicity	2.262	2.247	2.28	2.406	2.328	2.029	2.024	1.877	2.02	1.945	(12)
Hepatotoxicity	No	No	No	No	No	No	No	No	No	No	(5)
Skin sensitization	No	No	No	No	Yes	Yes	Yes	Yes	Yes	Yes	(5)
T. Pyriformis toxicity	0.45	0.533	0.628	0.894	0.462	0.171	0.515	0.175	0.189	0.008	(13)
Minnow toxicity	1.159	1.19	1.012	0.736	0.869	1.735	1.277	1.727	1.545	1.8	(14)

(1) log $mol.L^{-1}$; (2) log Papp (10^{-6} $cm.s^{-1}$); (3)%; (4) log Kp; (5) Yes/No; (6) log $L.kg^{-1}$; (7) log BB; (8) log PS; (9) log $mL.min^{-1}.kg^{-1}$; (10) log $mg.kg^{-1}.day^{-1}$; (11) $mol.kg^{-1}$; (12) log $mg.kg^{-1}\_bw.day^{-1}$; (13) log $\mu g.L^{-1}$; and (14) log mM

Table 7. ADMET properties of the studied compounds **11-19** and **D**

Property	11	12	13	14	15	16	17	18	19	D	Unit
Absorption											
Water solubility	-3.106	-3.377	-2.866	-3.377	-3.03	-2.544	-3.466	-6.011	-4.321	-2.47	(1)
$CaCo_2$ permeability	1.656	1.504	1.49	1.504	1.855	1.584	1.627	1.419	1.414	0.114	(2)
Intestinal absorption	94.81	95.31 7	92.78 8	95.31 7	95.36 6	94.98 8	94.9	96.18 3	95.66 9	59.90 1	(3)
Skin Permeability	-2.176	-2.413	-1.511	-2.413	-2.233	-2.693	-1.665	-1.456	-3.061	-2.735	(4)
P-glycoprotein substrate	No	No	No	No	No	No	No	No	No	Yes	(5)
P-glycoprotein I inhibitor	No	No	No	No	No	No	No	No	No	No	(5)
P-glycoprotein II inhibitor	No	No	No	No	No	No	No	No	No	No	(5)
Distribution											
VDss	0.27	0.166	0.17	0.166	0.307	-0.783	0.103	0.701	0.564	-1.905	(6)
Fraction unbound	0.373	0.42	0.447	0.42	0.412	0.438	0.395	0.18	0.327	0.328	(6)
BBB permeability	0.562	0.626	0.606	0.626	0.553	0.305	0.566	0.785	0.647	-0.864	(7)
CNS permeability	-2.226	-1.986	-2.159	-1.986	-2.399	-2.237	-2.199	-1.915	-2.521	-2.943	(8)
Metabolism											
CYP2D6 substrate	No	No	No	No	No	No	No	No	No	No	**(5)**
CYP3A4 substrate	No	No	No	No	No	No	No	No	No	No	**(5)**
CYP1A2 inhibitor	No	No	No	No	No	No	No	No	Yes	No	**(5)**
CYP2C19 inhibitor	No	No	No	No	No	No	No	No	Yes	No	**(5)**
CYP2C9 inhibitor	No	No	No	No	No	No	No	No	Yes	No	**(5)**
CYP2D6 inhibitor	No	No	No	No	No	No	No	No	No	No	**(5)**
CYP3A4 inhibitor	No	No	No	No	No	No	No	No	No	No	**(5)**
Excretion											
Total Clearance	0.945	0.376	0.437	0.376	1.029	0.978	0.587	1.202	0.905	0.197	**(9)**
Renal OCT_2 substrate	No	No	No	No	No	No	No	No	No	No	**(5)**
Toxicity											
AMES toxicity	No	No	No	No	No	No	No	No	No	No	**(5)**
Max. tolerated dose	0.479	0.543	0.65	0.543	0.526	0.312	0.474	0.193	0.148	0.692	**(10)**
hERG I inhibitor	No	No	No	No	No	No	No	No	No	No	**(5)**
hERG II inhibitor	No	No	No	No	No	No	No	No	No	No	**(5)**
Oral Rate Acute Toxicity	1.814	1.815	1.636	1.815	1.904	1.592	1.683	1.606	1.548	1.716	**(11)**
Oral Rate Chronic Toxicity	1.85	2.133	2.03	2.133	1.875	2.452	2.272	1.4	1.224	2.542	**(12)**
Hepatotoxicity	No	No	No	No	No	No	No	No	No	Yes	**(5)**
Skin Sensitization	Yes	Yes	Yes	Yes	Yes	Yes	Yes	Yes	Yes	No	**(5)**
T. Pyriformis toxicity	0.622	1.036	0.595	1.036	0.557	0.35	1.186	1.626	1.079	0.285	**(13)**
Minnow toxicity	1.643	0.945	1.213	0.945	1.593	1.059	0.604	0.088	0.955	3.698	**(14)**

(1) log $mol.L^{-1}$; **(2)** log Papp (10^{-6} $cm.s^{-1}$); **(3)**%; **(4)** log Kp; **(5)** Yes/No; **(6)** log $L.kg^{-1}$; **(7)** log BB; **(8)** log PS; **(9)** log $mL.min^{-1}.kg^{-1}$; **(10)** log $mg.kg^{-1}.day^{-1}$; **(11)** $mol.kg^{-1}$; **(12)** log $mg.kg^{-1}\_bw.day^{-1}$; **(13)** log $\mu g.L^{-1}$; and **(14)** log mM

The total essential oil is likely to have balanced plasma-tissue distribution given by the transitional range of logVDss; it is also predicted to cross the blood-brain barrier (logBB < -1) and penetrate the central nervous system (logPS < -3). Except for compound 19, there is no prediction on the interaction with the cytochromes P450 family (neither as the substrates nor the inhibitors); this equals no effects on liver activities. None of the compounds is likely to be excreted by organic cation transporter 2; this may help extend their in-body circulation and prolong their medicinal effects. In terms of toxicity, all the compounds are predicted to be considerably safe for medical use, such as: (i) no mutagenic potentials; (ii) no potential for fatal ventricular arrhythmia as hERG inhibitors; (ii) no hepatotoxicity; (iv) skin sensitization; and (v) toxicity to bacterium *T. Pyriformis* (pIGC50 >> -0.5) yet safety to animal organisms, *e.g.,* fish Flathead Minnows (LC_{50} >> -0.3). Overall, *D. orlowii* essential oil is considered as a suitable source for pharmacological developments.

Conclusion

This study is the first attempt to profile the antibacterial potentiality of *D. orlowii* essential oil against *S. pyogenes* and *S. pneumoniae* using a theory-experiment combinatory approach. Bioassays revealed the noticeably significant antibacterial activity against the two tested microorganism pathogens; the corresponding MICs values are 64 and 128 $\mu g.mL^{-1}$, respectively. Experimental extraction and GC-MS spectrometry characterized 19 compounds **1**-**19** in the oil-based extract, with the predominant contents of eucalyptol (**6**; 27.81%), *α*-citral (**14**; 17.13%), and *β*-citral (**12**; 13.91%). Molecular docking simulation expects all the candidates perform similarly upper-moderate inhibitory potentials toward the presentative structures for *lux*S proteins ($DS_{average}$ ca. 10 $kcal.mol^{-1}$). Quantum chemical calculation especially opts for **12** (4.56 D; 7.625 eV) and **14** (5.18 D; 7.614 eV) given by their both dipole-moment and electric-inducing advantages. Physicochemical analysis opts all the major components, **6** (154.3 amu; 18.9 $Å^3$; logP 2.81), **12** (152.3 amu; 18.4 $Å^3$; logP 2.56), and **14** (152.3 amu; 19.5 $Å^3$; logP 2.71), for their bio-medium compatibility based on Lipinski's rule of five and polarizability. ADMET analysis confirms the suitability and safety of all the candidates for pharmacological developments. Altogether, the results predict *D. orlowii* essential oil is a promising antibacterial source against the common respiratory bacteria, and encourage further testing on the major components (especially *α*-citral and *β*-citral).

Acknowledgments

This work was supported by Hue University under the Core Research Program [Project No. NCTB.DHH.2024.04]; and the L'Oreal-UNESCO For Women in Science International Award 2023.

Declaration of Interest

The authors declared that there was no financial conflict of interest was in this work. They also declared that the results/data/figures in this manuscript were not published, nor were they under consideration for publication elsewhere. The authors also declared that the mentioned information is true and correct. All the authors contributed to the study and the manuscript. If the manuscript is accepted for publication, the authors agree to transfer all copyright ownership of the manuscript to the Journal of Microbiology and Biotechnology, which covers the rights to use, reproduce, or distribute the article.

Ethical Approval

Ethical approval was not applicable for this article.

ORCID

Phan Tu Quy
https://orcid.org/0000-0002-5986-5944
Thanh Q. Bui
https://orcid.org/0000-0003-4076-4323
Nguyen Thi Thanh Hai
https://orcid.org/0000-0002-3603-4785
Tran Thi Ai My
https://orcid.org/0000-0003-3443-4328
Nguyen Duc Vu Quyen
https://orcid.org/0000-0002-1949-5379
Nguyen Vinh Phu
https://orcid.org/0000-0003-2389-3422
Nguyen Thanh Triet
https://orcid.org/0000-0001-6710-2448
Duong Phan Nguyen Duc
https://orcid.org/0000-0002-8143-3451
Ho Viet Duc
https://orcid.org/0000-0002-7442-3925
Nguyen Chi Bao
https://orcid.org/0000-0002-9239-3774
Ton That Huu Dat
https://orcid.org/0000-0002-6500-3363
Tran Nhat Phong Dao
https://orcid.org/0000-0002-5794-8447
Sunday Amos Onikanni
https://orcid.org/0000-0003-4866-8467
Nguyen Thi Ai Nhung
https://orcid.org/0000-0002-5828-7898

References

[1] Newman, M.F. *Distichochlamys*, a new genus from Vietnam. *Edinburgh Journal of Botany*, **1995**, 52(1), 65-69.
[2] Larsen, K. A new species of *Distichochlamys* from Vietnam and some observations on generic limits in Hedychieae (*Zingiberaceae*). *Natural History Bulletin of the Siam Society*, **2001**, 49, 77-80.
[3] Rehse, T., Kress, W. Distichochlamys rubrostriata (*Zingiberaceae*), a new species from northern Vietnam. *Brittonia*, **2003**, 55(3), 205-208.
[4] Nguyen, Q.B., Leong-Škorničková, J. *Distichochlamys benenica (Zingiberaceae*), a new species from Vietnam. *Gardens' Bulletin Singapore*, **2012**, 64(1),195-200.
[5] Pham, T.V., Hoang, H.N.T., Nguyen, H.T., Nguyen, H.M., Huynh, C.T., Vu, T.Y., *et al.* Anti-Inflammatory and Antimicrobial Activities of Compounds Isolated from *Distichochlamys benenica*. *BioMed Research International*, **2021**, 2021, 6624347.
[6] Hoang, H.T.N., Dinh, T.T.T., Pham, T.V., Le, H.B.T., Ho, D.V. Chemical composition and acetylcholinesterase inhibitory activity of essential oil from rhizomes of *Distichochlamys benenica*. *Hue University Journal of Science: Natural Science*, **2020**, 129(1D), 43-49.
[7] Tran, B.G., Do, H.B., Dinh, H.N.Q., Nguyen, P.H., Dao, K.K., Pham, T.V. Evaluation of the anti-inflammatory activity of the rhizome essential oil of Distichochlamys citrea. *HO CHI MINH CITY Open University Journal of Science- Engineering and Technology*, **2025**, 15(2), 65–75.
[8] Pham, T.V., Hoang, H.N.T., Nguyen, H.T., Nguyen, H.M., Huynh, C.T., Vu, T.Y., Do, A.T., Nguyen, N.H., Do, B.H., Ogunwande, I.O. Volatile constituents of *Distichochlamys citrea* MF Newman and *Distichochlamys orlowii* K. Larsen MF Newman (*Zingiberaceae*) from Vietnam. *Journal of Medicinal Plants Research*, **2017**, 11, 188-193.
[9] Tran-Trung, H., Vu, D.C., Van Trung, H., Hoang Tuan, N., Thang, T.D., Nguyen, T.H. Assessing enzymatic inhibitory effects of essential oil from *Distichochlamys orlowii* K. Larsen & MF Newman rhizomes. *Journal of Biologically Active Products from Nature*, **2023**, 13(6), 562-572.
[10] Nguyen, X.T., Nguyen, T.H., Le Thi, H., Nguyen, T.V.A., Le Hong, L. Quantification of Total Polyphenols, Total Flavonoids, and Evaluation of Antioxidant Activity of the Aerial Part of *Distichochlamys orlowii* K. Larsen & MF Newman. *VNU Journal of Science: Medical and Pharmaceutical Sciences*, **2023**, 39(4), 55-63.
[11] Shulman, S.T., Bisno, A.L., Clegg, H.W., Gerber, M.A., Kaplan, E.L., Lee, G., *et al.* Clinical practice guideline for the diagnosis and management of group A streptococcal pharyngitis: 2012 update by the infectious diseases Society of America. *Clinical Infectious Diseases*, **2012**; 55(10), e86-e102.
[12] Avire, N.J., Whiley, H., Ross, K. A review of *Streptococcus pyogenes*: public health risk factors, prevention and control. *Pathogens*, **2021**; 10(2):248.
[13] Van de Beek, D., de Gans, J., Tunkel, A.R., Wijdicks, E.F. Community-acquired bacterial meningitis in

adults. *New England Journal of Medicine*, **2006**; 354(1), 44-53.
[14] Song, S., Wood, T.K. The primary physiological roles of autoinducer 2 in *Escherichia coli* are chemotaxis and biofilm formation. *Microorganisms*, **2021**, 9(2), 386.
[15] Lyon, W.R., Madden, J.C., Levin, J.C., Stein, J.L. Caparon MG. Mutation of luxS affects growth and virulence factor expression in *Streptococcus pyogenes*. *Molecular Microbiology*, **2001**, 42(1), 145-57.
[16] Kang, S.O., Caparon, M.G., Cho, K.H. Virulence gene regulation by CvfA, a putative RNase: the CvfA-enolase complex in *Streptococcus pyogenes* links nutritional stress, growth-phase control, and virulence gene expression. *Infection and Immunity*, **2010**, 78(6), 2754-2767.
[17] Thao, T.T.P., Bui, T.Q., Quy, P.T., Bao, N.C., Van Loc, T., Van Chien, T., *et al.* Isolation, semi-synthesis, docking-based prediction, and bioassay-based activity of *Dolichandrone spathacea* iridoids: new catalpol derivatives as glucosidase inhibitors. *RSC Advances*, **2021**, 11(20), 11959-11975.
[18] Thao, T.T.P., Bui, T.Q., Hai, N.T.T., Huynh, L.K., Quy, P.T., Bao, N.C., *et al.* Newly synthesised oxime and lactone derivatives from *Dipterocarpus alatus* dipterocarpol as anti-diabetic inhibitors: experimental bioassay-based evidence and theoretical computation-based prediction. *RSC Advances*, **2021**, 11(57), 35765-35782.
[19] Institute CaLS. Performance Standards for Antimicrobial Susceptibility Testing - M100, 33rd ed. *Pennsylvania: A CLSI Supplement for Global Application*, **2023**.
[20] ULC, C. Molecular operating environment (MOE), 2020.09, 1010 Sherbooke St. West, Suite. **2022**, 910.
[21] Caricato, M., Frisch, M.J., Hiscocks, J., Frisch, M.J. Gaussian 09: IOps Reference. *Gaussian Wallingford, CT, USA*, **2009**.
[22] Zhao, Y., Schultz, N.E., Truhlar, D.G. Design of density functionals by combining the method of constraint satisfaction with parametrization for thermochemistry, thermochemical kinetics, and noncovalent interactions. *Journal of Chemical Theory and Computation*, **2006**, 2(2), 364-382
[23] Reed, A.E., Weinstock, R.B., Weinhold F. Natural population analysis. *The Journal of Chemical Physics*, **1985**, 83(2), 735-746.
[24] Mignani, S., Rodrigues, J., Tomas, H., *et al.* Present drug-likeness filters in medicinal chemistry during the hit and lead optimization process: how far can they be simplified? *Drug Discov Today*, **2018**, 23(3), 605-615.
[25] Gasteiger, J., Marsili, M. Iterative partial equalization of orbital electronegativity—a rapid access to atomic charges. *Tetrahedron*, **1980**, 36(22), 3219-3228.
[26] Lipinski, C.A., Lombardo, F., Dominy, B.W., Feeney, P.J. Experimental and computational approaches to estimate solubility and permeability in drug discovery and development settings. *Advanced Drug Delivery Reviews*, **1997**, 23(1-3), 3-25.
[27] Ahsan, M.J., Samy, J.G., Khalilullah, H., Nomani, M.S., Saraswat, P., Gaur, R., *et al.* Molecular properties prediction and synthesis of novel 1, 3, 4-oxadiazole analogues as potent antimicrobial and antitubercular agents. *Bioorganic & Medicinal Chemistry Letters*, **2011**, 21(24), 7246-7250.
[28] Mazumder, A., Chakraborty, R., Sen, S., Vadra, B., De, B., Ravi, T. Synthesis and biological evaluation of some novel quinoxalinyl triazole derivatives. *Der Pharma Chem*, **2009**, 1(2), 188-198.
[29] Pires, D.E., Blundell, T.L., Ascher, D.B. pkCSM: predicting small-molecule pharmacokinetic and toxicity properties using graph-based signatures. *Journal of Medicinal Chemistry*, **2015**, 58(9), 4066-4072.
[30] Murata, S., Shiragami, R., Kosugi, C., Tezuka, T., Yamazaki, M., Hirano, A., *et al.* Antitumor effect of 1, 8-cineole against colon cancer. *Oncology Reports*, **2013**, 30(6), 2647-2652.
[31] Dammak, I., Hamdi, Z., El Euch, S.K., Zemni, H., Mliki, A., Hassouna, M., *et al.* Evaluation of antifungal and anti-ochratoxigenic activities of *Salvia officinalis, Lavandula dentata* and *Laurus nobilis* essential oils and a major monoterpene constituent 1, 8-cineole against *Aspergillus carbonarius. Industrial Crops and Products*, **2019**, 128, 85-93.
[32] Schürmann, M., Oppel, F., Gottschalk, M., Büker, B., Jantos, C.A., Knabbe, C., *et al.* The therapeutic effect of 1, 8-cineol on pathogenic bacteria species present in chronic rhinosinusitis. *Frontiers in Microbiology*, **2019**, 10, 2325.
[33] Pham, T.V., Truong, V., Dang, N.T.T., Vo, Q.H., Ho, D.V. Chemical composition of the essential oils of Distichochlamys citrea leaves collected from Central Vietnam. *Vietnam Journal of Chemistry*, **2017**, 55(4E23), 358–362.
[34] Chau, D. T., Hung, N. V., Dai, D. N., Ogunwande, I. A. Volatile constituents of Distichochlamys citrea MF Newman and Distichochlamys orlowii K. Larsen MF Newman (Zingiberaceae) from Vietnam. *Journal of Medicinal Plants Research*, **2017**, 11(9), 188-193.
[35] Jirovetz, L., Buchbauer, G., Puschmann, C., Fleischhacker, W., Shafi, P.M., Rosamma, M. Analysis of the essential oil of the aerial parts of the medicinal plant *Aristolochia indica* Linn.(*Aristolochiaceae*) from South-India. *Scientia Pharmaceutica*, **2000**, 68(3), 309-316.

[36] Govindachari, T., Mohamed, P., Parthasarathy, P. Ishwarane and aristolochene, two new sesquiterpene hydrocarbons from *Aristolochia indica*. *Tetrahedron*, **1970**, 26(2), 615-619.
[37] Van Hue, N., Cuong, T.D., Quy, P.T., Bui, T.Q., Hai, N.T.T., Triet, N.T., *et al.* Antimicrobial properties of *Distichochlamys citrea* MF Newman rhizome n-hexane extract against *Streptococcus pyogenes*: experimental evidences and computational screening. *Chemistry Select*, **2022**, 7(17), e202200680.
[38] Thai, N.M., Bui, T.Q., Quy, P.T., Thanh Hai, N.T., To, D-C., Quang, D.T., *et al.* Potentiality of Organosulfur Compounds Against SARS-CoV-2-Coinfected Bacteria *Streptococcus pyogenes* and *S pneumoniae*: A Cross-Platform Analysis from Computational Chemistry. *Natural Product Communications*, **2023**, 18(8).
[39] Loan, H.T.P., Bui, T.Q., My, T.T.A., Hai, N.T.T., Quang, D.T., Tat, P.V., *et al.* In-Depth investigation of a donor–acceptor interaction on the heavy-group-14@group-13-diyls in transition-metal tetrylone complexes: Structure, bonding, and property. *ACS Omega*, **2020**, 5(33), 21271-21287.
[40] Ayers, P.W., Yang, W., Bartolotti, L.J. 18 Fukui Function. *Chemical Reactivity Theory*, **2010**; 255
[41] Fukui, K., Yonezawa, T., Shingu, H. A molecular orbital theory of reactivity in aromatic hydrocarbons. *The Journal of Chemical Physics*, **1952**, 20(4), 722-725.
[42] Rosenberg, B. Electrical conductivity of proteins. *Nature*, **1962**, 193(4813), 364-365.
[43] Kharkyanen, V., Petrov, E., Ukrainskii, I. Donor-acceptor model of electron transfer through proteins. *Journal of Theoretical Biology*, **1978**, 73(1), 29-50.
[44] Gray, H.B., Winkler, J.R. Electron transfer in proteins. *Annual Review of Biochemistry*, **1997**, 65(1), 537-561.
[45] Feynman, R.P. The Feynman lectures on physics. *Addison–Wesley, USA*, **1963**; 1, 46.

HOW TO CITE THIS MANUSCRIPT
P.T. Quy, T.Q. Bui, N.T.T. Hai, T.T.A. My, N.D.V. Quyen, N.V. Phu, N.T. Triet, D.P. Nguyen Duc, H.V. Duc, N.C. Bao, T.T.H. Dat, T.N.P. Dao, S.A.BOnikanni, N.T.A. Nhung. Antibacterial Activity of *Distichochlamys Orlowii* K. Larsen and M. F. Newman Essential Oil against *Streptococcus pyogenes* and *Streptococcus Pneumoniae*: *In Vitro* Evidence and *In Silico* Prediction. *Asian Journal of Green Chemistry*, 10 (4) 2026, 756-778.
DOI: https://doi.org/10.48309/AJGC.2026.561172.1878
URL: https://www.ajgreenchem.com/article_242056.html